

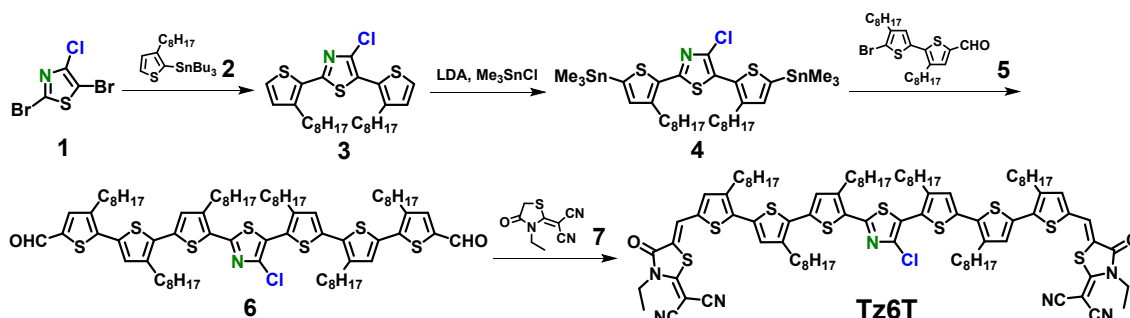
## Supporting Information

### **Simple Thiazole-Centered Oligothiophene Donor with 15.4% Efficiency in All Small Molecule Organic Solar Cells**

Tainan Duan, Qianqian Chen, Qianguang Yang, Dingqin Hu, Guilong Cai, Xinhui Lu, Jie Lv, Hang Song, Cheng Zhong, Feng Liu, Donghong Yu, and Shirong Lu

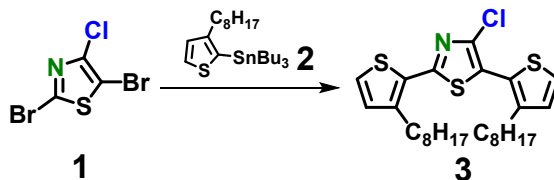
# Experimental Procedures

## 1. Synthetic protocols



**Scheme S1.** Synthesis of the donors **Tz6T**.

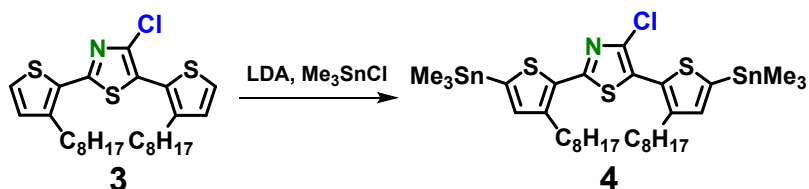
Note: Compounds 2,5-dibromo-4-chlorothiazole (**1**)<sup>1</sup> and 5'-bromo-3,4'-dioctyl-[2,2'-bithiophene]-5-carbaldehyde (**5**)<sup>2</sup> were prepared according to previously report procedures.



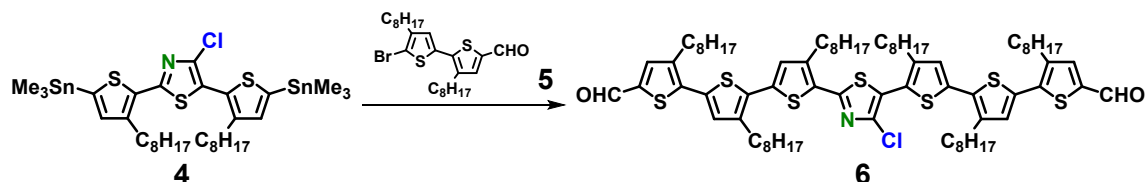
**4-chloro-2,5-bis(3-octylthiophen-2-yl)thiazole (3):** In a pre-dried Schlenk tube, 2,5-dibromo-4-chlorothiazole (**1**) (1.00 g, 3.60 mmol), tributyl(3-octylthiophen-2-yl)stannane (**2**) (3.85 g, 7.93 mmol) and Pd(PPh<sub>3</sub>)<sub>4</sub> (416 mg, 0.36 mmol) were dissolved in pre-degassed toluene (60 mL). The reaction mixture was heated to 120 °C and was stirred for 48 h. Next, the mixture was concentrated under reduced pressure. The crude product was purified by column chromatography over SiO<sub>2</sub> using hexanes/CH<sub>2</sub>Cl<sub>2</sub> (10:1) as the eluent. The solvent was removed by rotary evaporation, affording desired compound **3** as a pale yellow oil (1.50 g, yield: 82%).

<sup>1</sup>H NMR (400 MHz, CDCl<sub>3</sub>, δ ppm): 7.40 (d, *J* = 5.2 Hz, 1H), 7.33 (d, *J* = 5.2 Hz, 1H), 7.00 (d, *J* = 5.2 Hz, 1H), 6.97 (d, *J* = 5.2 Hz, 1H), 2.91 (t, *J* = 7.8 Hz, 1H), 2.64 (t, *J* = 7.8 Hz, 1H), 1.73-1.55 (m, 4H), 1.43-1.24 (m, 20H), 0.89-0.83 (m, 6H). <sup>13</sup>C NMR (100 MHz, CDCl<sub>3</sub>, δ ppm): 159.88, 144.22, 143.42, 138.07, 130.66, 130.56, 129.08, 127.30, 127.00,

123.21, 122.02, 31.87, 30.50, 30.03, 29.91, 29.61, 29.44, 29.41, 29.38, 29.24, 22.66, 14.08.



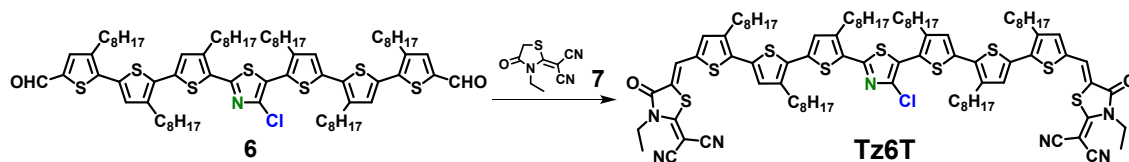
**4-chloro-2,5-bis(3-octyl-5-(trimethylstannyl)thiophen-2-yl)thiazole (4):** In a pre-dried Schlenk tube, a solution of compound **3** (1.02 g, 2.0 mmol) in anhydrous THF (40 mL) was cooled to -78 °C. A solution of LDA (1.0 M in THF, 5.2 mL, 5.2 mmol) was added dropwise, and the mixture was stirred for 2 h at -78 °C. Next, trimethyltin chloride in THF (1.0 M, 6.0 mL, 6.0 mmol) was added to the mixture in one portion. The cooling bath was then removed, the mixture was allowed to warm to room temperature, and was stirred for another 3 h. The reaction was quenched with saturated KF solution (30 mL) and the aqueous phase was extracted with dichloromethane (2 × 50 mL). The organic phase was collected, dried over Na<sub>2</sub>SO<sub>4</sub>, concentrated under reduced pressure, and compound **4** was obtained as a pale yellow oil used in the next step without the need for further purification (1.56 g, yield: 93%)



**5',5''''-(4-chlorothiazole-2,5-diyl)bis(3,4',4''-trioctyl-[2,2':5',2''-terthiophene]-5-carbaldehyde) (6):** In a pre-dried Schlenk tube, organotin **4** (833 mg, 1.0 mmol.), aldehyde **5** (1.19 g, 2.4 mmol) and Pd(PPh<sub>3</sub>)<sub>4</sub> (115 mg, 0.1 mmol) were dissolved in pre-degassed toluene (40 mL). The reaction mixture was heated to 120 °C and was stirred for 48 h. Next, the mixture was concentrated under reduced pressure. The crude product was purified by column chromatography over SiO<sub>2</sub> using hexanes/CHCl<sub>3</sub> (2:3) as the eluent. The solvent was removed by rotary evaporation, affording desired compound **6** as an orange-red solid (1.41 g, 88%).

<sup>1</sup>H NMR (400 MHz, CDCl<sub>3</sub>, δ ppm): 9.83 (s, 2H), 7.59 (s, 2H), 7.16-7.10 (m, 2H), 7.06-7.05 (m, 2H), 2.90-2.78 (m, 10H), 2.67 (t, *J* = 7.2 Hz, 2H), 1.70-1.68 (m, 10H), 1.42-1.28

(m, 60H), 0.88, 0.87 (m, 12H).  $^{13}\text{C}$  NMR (100 MHz,  $\text{CDCl}_3$ ,  $\delta$  ppm): 182.45, 159.12, 144.59, 143.91, 141.31, 141.01, 140.82, 140.72, 140.64, 140.50, 140.41, 140.31, 138.93, 138.21, 137.22, 136.73, 133.50, 133.12, 132.37, 132.22, 130.60, 130.51, 129.19, 128.01, 123.70, 121.65, 31.89, 31.88, 30.53, 30.51, 30.37, 30.29, 30.23, 29.80, 29.68, 29.55, 29.50, 29.46, 29.44, 29.41, 29.28, 29.25, 22.68, 14.09.



**2,2'-((5Z,5'Z)-(((4-chlorothiazole-2,5-diyl)bis(3,4',4''-trioctyl-[2,2':5',2''-terthiophene]-5'',5-diyl))bis(methanylylidene))bis(3-ethyl-4-oxothiazolidine-5,2-**

**diylidene))dimalononitrile (Tz6T):** The aldehyde **6** (268 mg, 0.2 mmol), 2-(3-ethyl-4-oxothiazolidin-2-ylidene)malononitrile (**7**) (193 mg, 1.0 mmol) and ammonium acetate (200 mg) were added into a mix solution of chloroform/acetic acid (10 mL/20 mL), and the mixture was heated to 100 °C and stirred for 6 h. The reaction mixture was allowed to cool down to room temperature, filtered, and washed with methanol (2 × 20 mL) and ethyl acetate (2 × 20 mL), affording the desired products as a purple-black solid in high yield and high purity (308 mg, 91%). Further purification can be simply performed *via* recrystallization in ethyl acetate.

$^1\text{H}$  NMR (400 MHz,  $\text{CHCl}_3$ ,  $\delta$  ppm): 8.00 (s, 2H), 7.30 (s, 2H), 7.19 (m, 2H), 7.10 (s, 1H), 7.08 (s, 2H), 4.35 (q,  $J = 7.2$  Hz, 4H), 2.93-2.81 (m, 10H), 2.68 (t,  $J = 7.6$  Hz, 4H), 1.80-1.62 (m, 12H), 1.43-1.28 (m, 66H), 0.88-0.86 (m, 12H).  $^{13}\text{C}$  NMR(100 MHz,  $\text{CHCl}_3$ ,  $\delta$  ppm): 165.92, 165.60, 159.06, 144.65, 143.98, 141.62, 141.45, 141.00, 140.88, 140.66, 138.80, 138.23, 137.13, 136.64, 134.02, 133.90, 133.05, 132.74, 132.64, 132.56, 130.70, 129.27, 128.65, 128.08, 123.83, 121.67, 113.66, 113.54, 113.32, 112.29, 55.70, 55.65, 40.70, 31.89, 31.87, 30.67, 30.55, 30.51, 30.22, 29.83, 29.71, 29.65, 29.62, 29.53, 29.51, 29.46, 29.42, 29.33, 29.28, 29.26, 22.68, 14.21, 14.10. HR-MS (+APCI,  $m/z$ ): calcd. for  $\text{C}_{93}\text{H}_{121}\text{ClN}_7\text{O}_2\text{S}_9^+$   $[\text{M}+\text{H}]^+$ : 1690.67512, found 1690.67163.

## 2. Device fabrications and Testing

The device structures were ITO/PEDOT:PSS/Active layer/Phen-NaDPO/Ag. ITO coated glass substrates were cleaned with detergent water, deionized water, acetone and isopropyl alcohol in an ultrasonic bath sequentially for 15 min, and further treated with UV exposure for 15 min in a UV-ozone chamber. A thin layer (ca. 30 nm) of PEDOT:PSS (Bayer Baytron 4083) was first spin-coated on the substrates with 4000 rpm and baked at 150 °C for 10 min under ambient conditions. The substrates were then transferred into a nitrogen-filled glove box. The all optimized concentration was 18 mg/ml chloroform solution with D:A ratio of 1.8:1 (w/w). After spin coating, the 2Cl7T:eC9-4F blend film was annealed at 120 °C for 5 mins. And the Tz6T:eC9-4F blend film was annealed at 150 °C for 5 mins. Then Phen-NaDPO as the electron transporting layer was spin-coated on the active layer by 2000 rpm from isopropyl alcohol solution. Finally, the substrates were transferred to a thermal evaporator, and top electrode was evaporated at a pressure of  $2 \times 10^{-5}$  Pa.

The external quantum efficiency (EQE) was performed using certified IPCE equipment (Zolix Instruments, Inc, Solar Cell Scan 100). The  $J-V$  curves were measured under AM 1.5 G ( $100 \text{ mW cm}^{-2}$ ) (Enli Technology Co., Ltd. SS-X50R). The  $J-V$  measurement signals were recorded by a Keithley 2400 source-measure unit. Device area of each cell was  $0.08636 \text{ cm}^2$ .

## 3. Instruments and Characterizations

**Material characterization:** NMR spectra ( $^1\text{H}$  and  $^{13}\text{C}$ ) were recorded on on Bruker Avance III Ultrashield Plus instruments (400 MHz) spectrometer. Matrix-Assisted Laser Desorption/Ionization Time of Flight Mass Spectrometry (MALDI-TOF-MS) data of Tz6T was collected by using a Bruker ultrafleXtreme MALDI-TOF/TOF mass spectrometer. 2Cl7T, Tz6T and eC9-4F were purified by preparative-scale recycling size-exclusion chromatography (SEC) on an LC-9160NEXT (JAI) system prior to being examined as SM donor/acceptor in ASM-OSCs.

**Thermal analyses:** The measurements of Thermogravimetric Analysis (TGA) and Differential Scanning Calorimetry (DSC) were performed on a Mettler-Toledo TGA/DSC 3+ analyzer under a nitrogen atmosphere, using aluminum crucibles.

**Photophysical and electrochemical property characterizations:** UV-vis spectra (solution and film) were recorded on a PerkinElmer LAMBDA 365 UV-Vis spectrophotometer. Cyclic Voltammetry (CV) was performed with a CHI660e electrochemical workstation, using a glassy carbon button electrode as the working electrode, a platinum wire as the auxiliary electrode, and an Ag/Ag<sup>+</sup> glass electrode as the reference electrode. The Ag/Ag<sup>+</sup> reference electrode was calibrated using the ferrocene/ferrocenium (Fc/Fc<sup>+</sup>) redox couple. Fc/Fc<sup>+</sup> is taken to be 4.8 eV relative to the vacuum level. All the CV curves were measured by casting the thin film (from CHCl<sub>3</sub> solution of SM materials) on the glassy carbon electrode.

**Contact Angle Measurements:** The contact angles of two different solvents (water and formamid) on the neat films (donor/acceptor) were measured on a DSA-100 drop shape analyzer (KRÜSS Scientific). The miscibility of two components in the blend can be estimated from the solubility parameters ( $\delta$ ) of each material, which can be calculated with equation:  $\delta = K\sqrt{\gamma}$ , Where  $\gamma$  is the surface energy of the material, and  $K$  is the proportionality constant ( $K = 116 \times 10^3 \text{ m}^{1/2}$ ).

**Space charge limited current (SCLC) measurements:** The carrier mobility (hole and electron mobility) of photoactive active layer was obtained by fitting the dark current of hole/electron-only diodes to the space-charge-limited current (SCLC) model. Hole-only diode configuration: ITO/PEDOT:PSS/active layer/MoO<sub>3</sub>/Ag; here,  $V_{bi} = 0 \text{ V}$  (flat band pattern formed by MoO<sub>3</sub>-MoO<sub>3</sub>). Electron-only diode configuration: ITO/ZnO/Phen-NaDPO/active layer/Phen-NaDPO/Ag; here,  $V_{bi} = 0\text{V}$  was used following the protocol reported.<sup>3</sup> The active layer thickness was determined by a Tencor surface profilometer. The electric-field dependent SCLC mobility was estimated using the following equation:

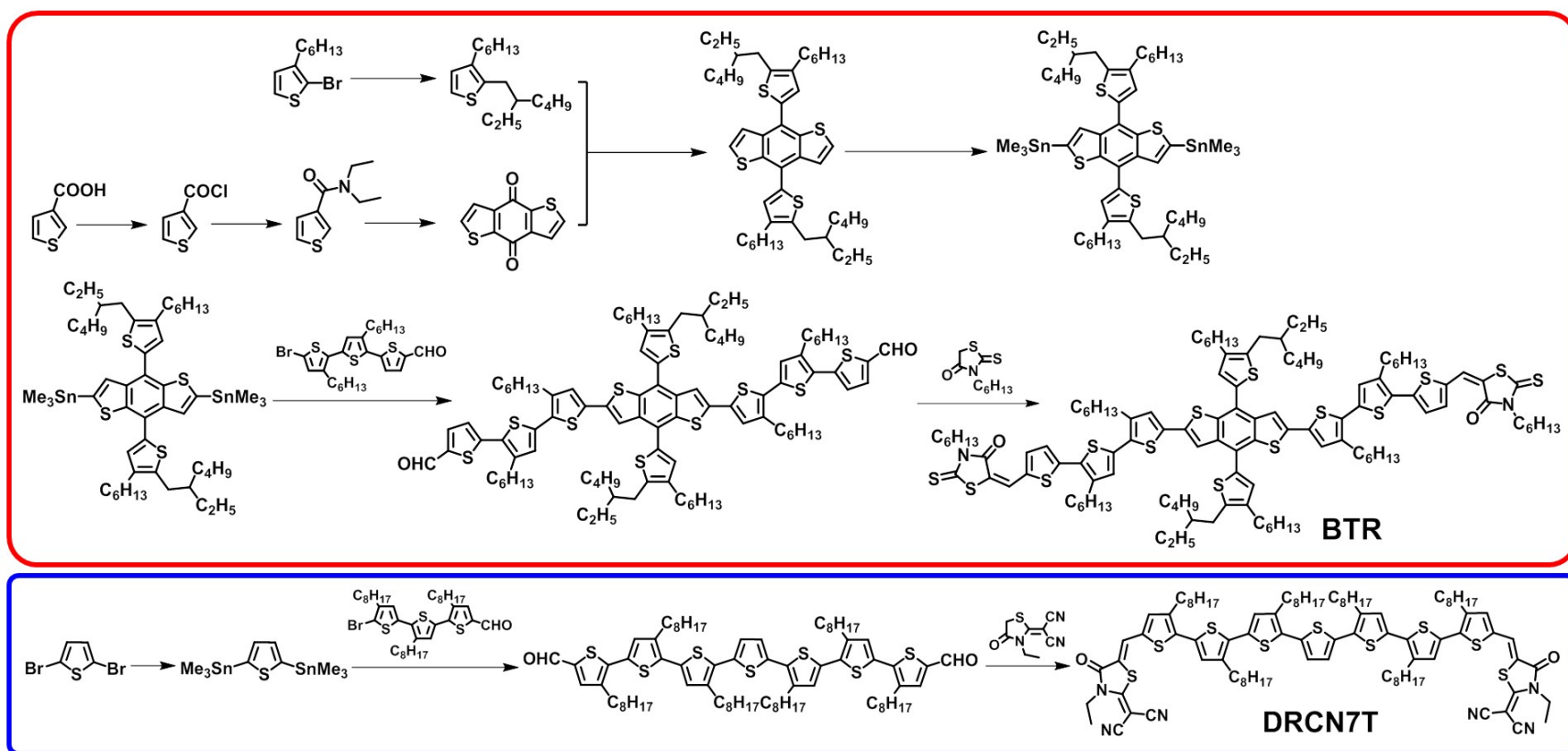
$$J(V) = \frac{9}{8} \varepsilon_0 \varepsilon_r \mu_0 \exp\left(0.89\beta \sqrt{\frac{V - V_{bi}}{L}}\right) \frac{(V - V_{bi})^2}{L^3}$$

**Atomic force microscopy (AFM) measurements:** Topographic images of the films were obtained from a Bruker atomic force microscopy (AFM) with the type of dimension

edge with Scan Asyst™ in the tapping mode using an etched silicon cantilever at a nominal load of  $\sim 2\text{nN}$ , and the scanning rate for a  $2\ \mu\text{m} \times 2\ \mu\text{m}$  image size was 1.5 Hz.

**Grazing incidence wide-angle X-ray scattering (GIWAXS):** GIWAXS measurements with  $K\alpha$  X-ray of Cu source (8.05 KeV, 1.54 Å) and a Pilatus3R 300 K detector were conducted at a Xeuss 2.0 SAXS/WAXS laboratory beamline. Si substrates were sonicated for 15 min in turn in successive baths of acetone and isopropanol. The substrates were then dried with pressurized nitrogen before being exposed to the UV-ozone plasma for 15 min. Then the samples were prepared by spin coating identical chloroform blend solutions as those used in ASM-OSCs on Si substrates. The grazing incident angle was  $0.15^\circ$ .

## Schemes, Figures and Tables



Scheme S2. Synthetic routes of SM donors BTR and DRCN7T

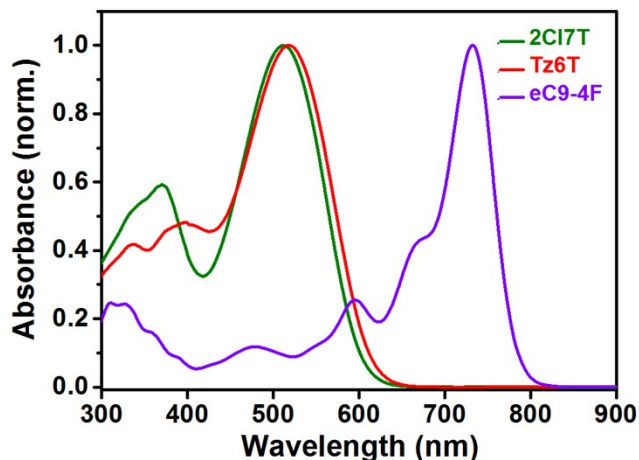


Figure S1. Normalized UV-vis spectra of SM donors and acceptor in chloroform solution.

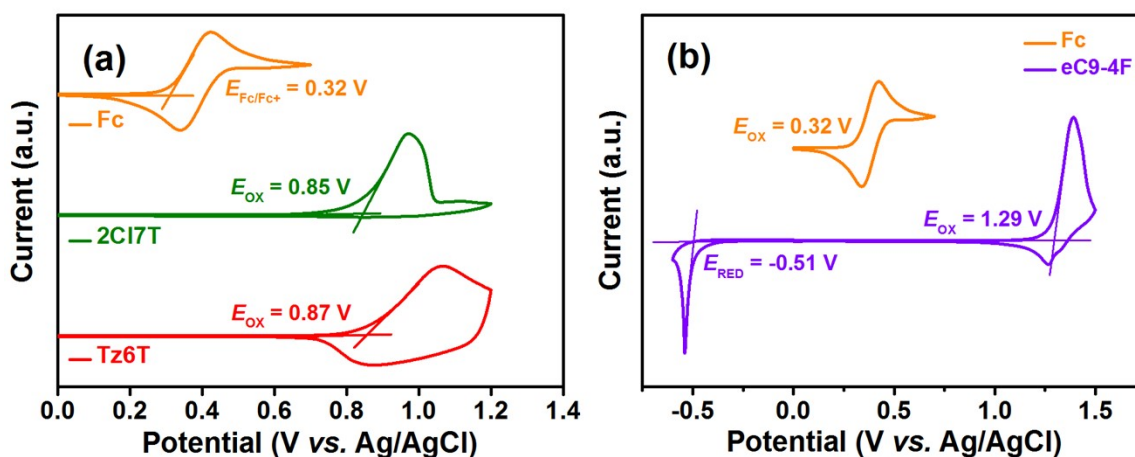


Figure S2. (a) Oxidation scans of the SM donor vs. Fc/Fc<sup>+</sup>; (b) Oxidation and reduction scans of SM acceptor eC9-4F vs. Fc/Fc<sup>+</sup>.

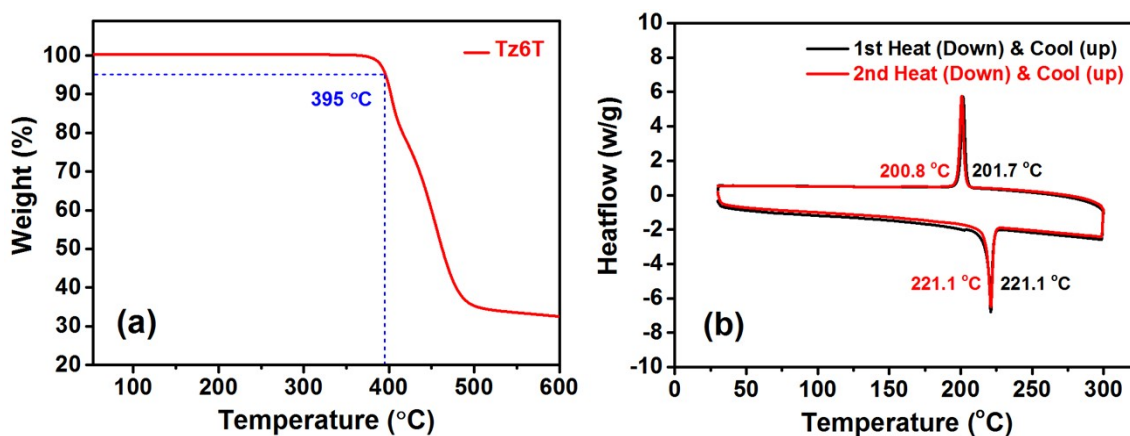
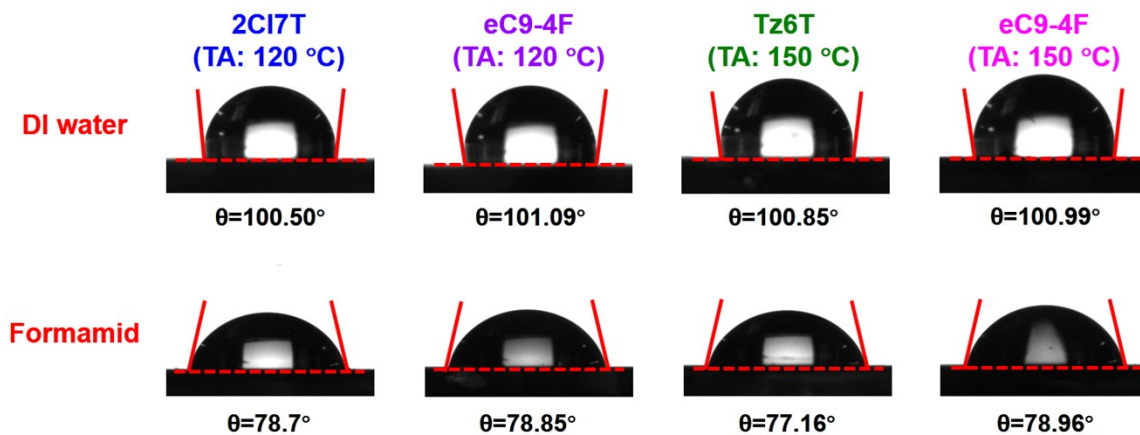
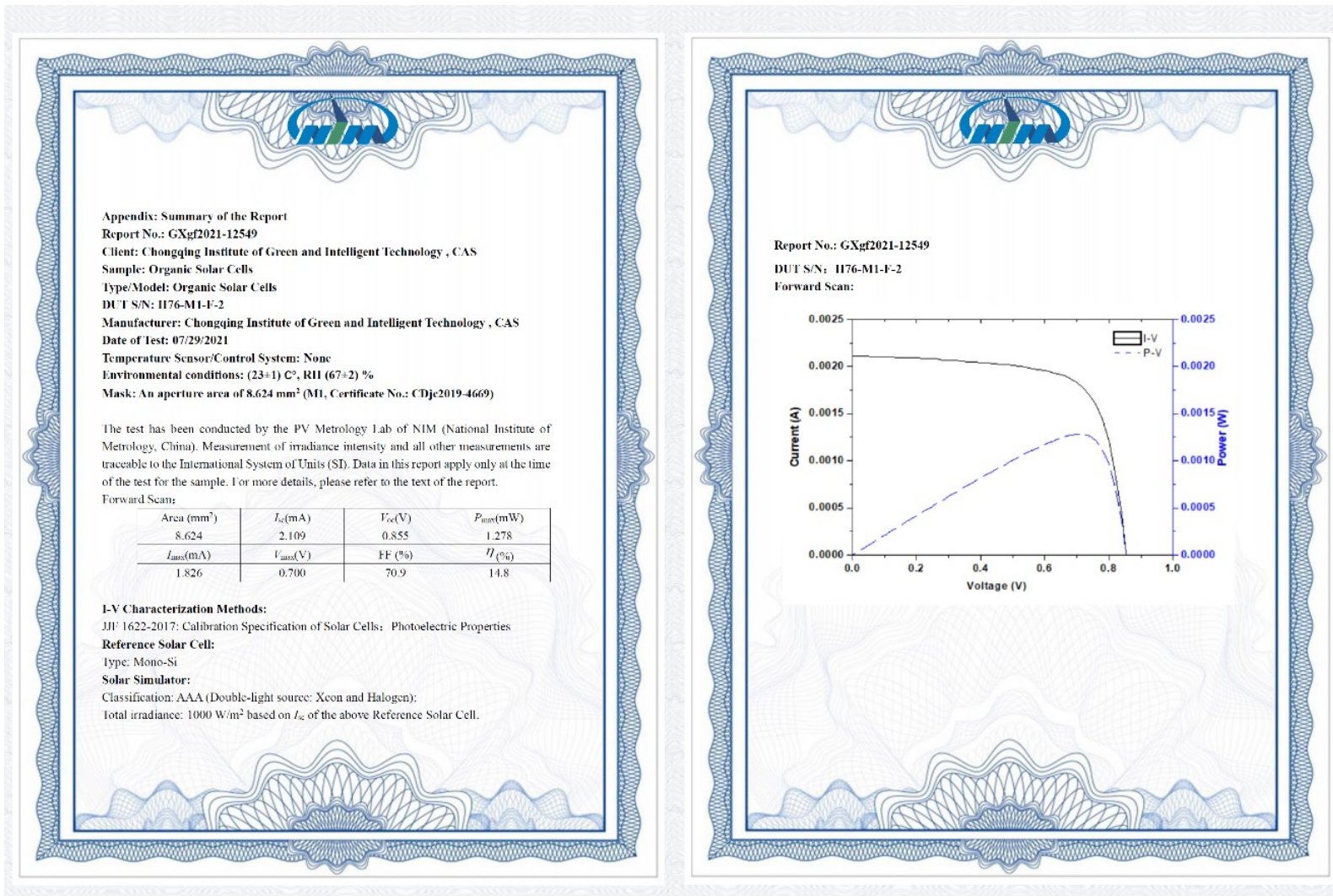


Figure S3. (a) Thermogravimetric analysis (TGA) of Tz6T under nitrogen atmosphere with heating rate of 10 °C/min; (b) Differential Scanning Calorimetry (DSC) traces of Tz6T. Analyses carried out with a scan rate of 10 °C/min between 30 °C and 300 °C



**Figure S4.** Contact angle with deionized water and formamid of 2CI7T, Tz6T and eC9-4F films. The temperature of thermal annealing (TA) is determined by the optimized post-treatment conditions of 2CI7T:eC9-4F and Tz6T:eC9-4F blends, respectively.



**Figure S5.** Report of certified efficiency of the optimized Tz6T:cC9-4F binary single junction solar cells, measured by National Institute of Metrology (NIM), China.

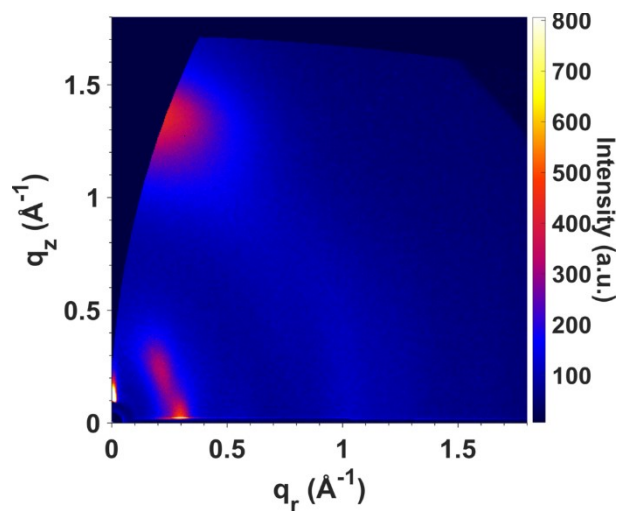


**Figure S6.** 2D GIWAXS pattern of the neat film of eC9-4F.

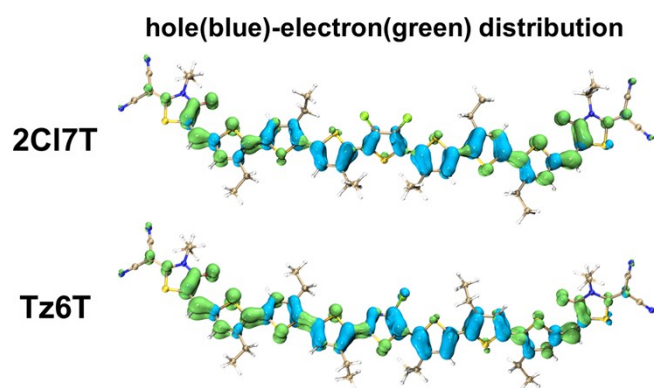


**Figure S7.** Hole(blue)-electron(green) distribution of **2CI7T** and **Tz6T** calculated at relaxed S1 state.

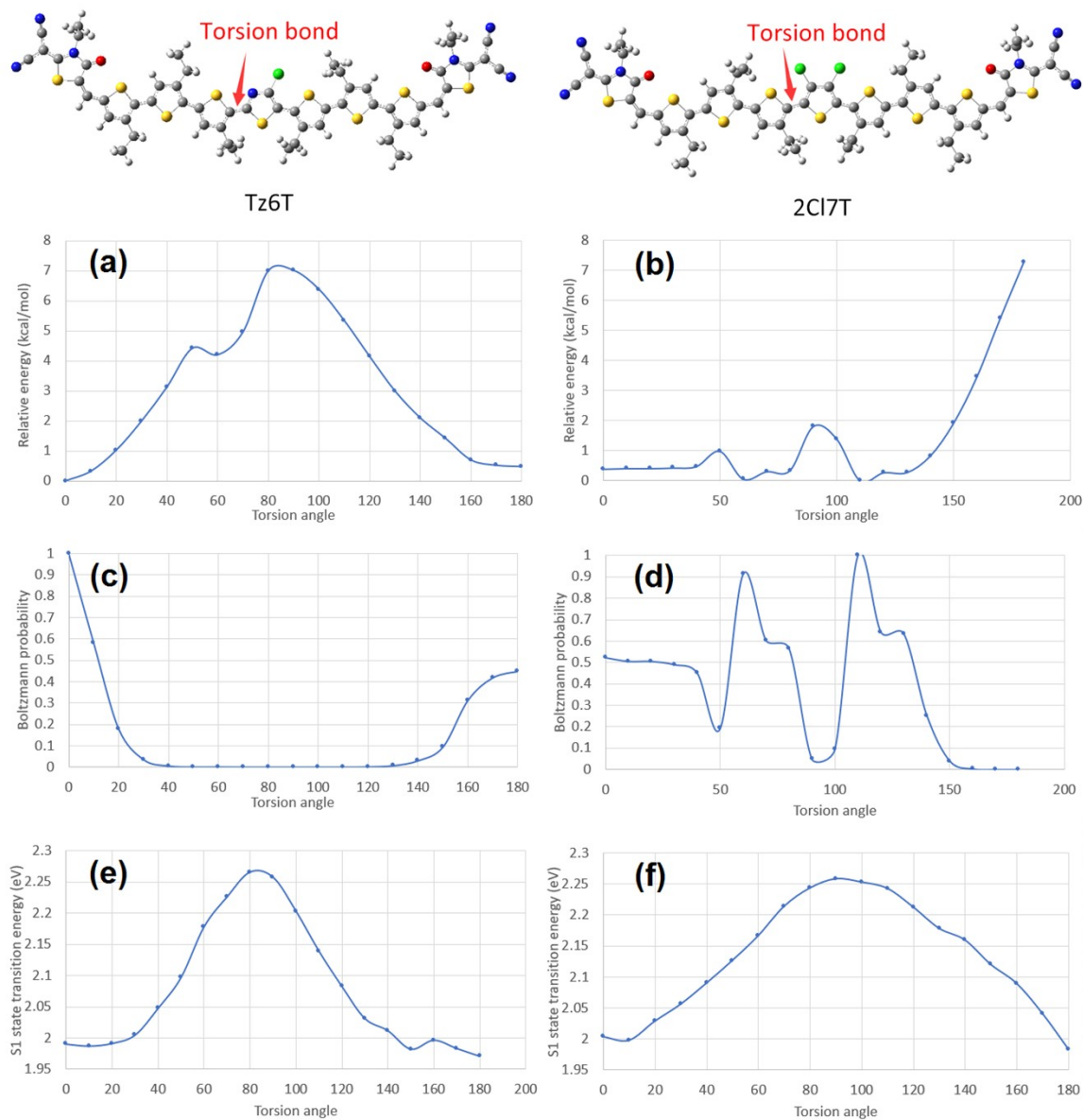


**Figure S8.** (a,b) Ground state relative energy versus torsion angle. (c,d) Boltzmann probability versus torsion angle. (e,f) S1 state transition versus torsion angle.

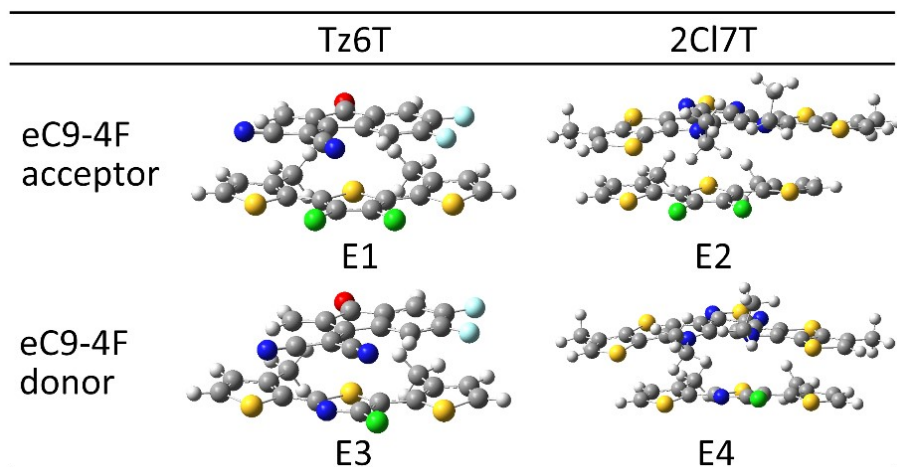


**Figure S9.** Optimized interaction conformation between central donor unit (central three five-member ring) of **Tz6T/2Cl7T** and donor/acceptor moiety of **eC9-4F**. The initial geometry was obtained by conformation search with Molclus/genmer program. The relative stacking energy is obtained by  $E_{\text{stack}} = (E1-E3) - (E2-E4)$ .

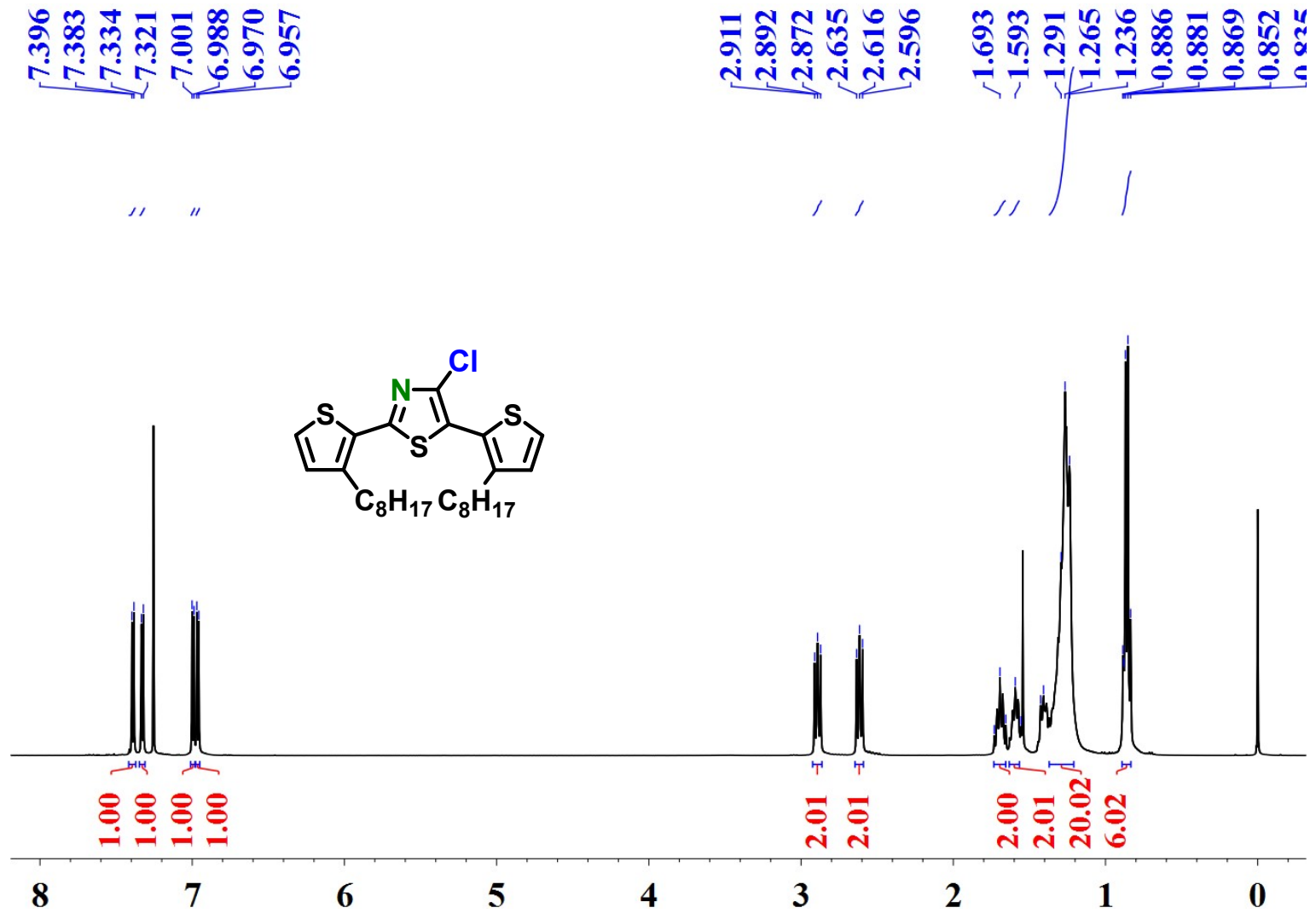


Figure S10. <sup>1</sup>H NMR spectrum of compound 3 in CDCl<sub>3</sub>.

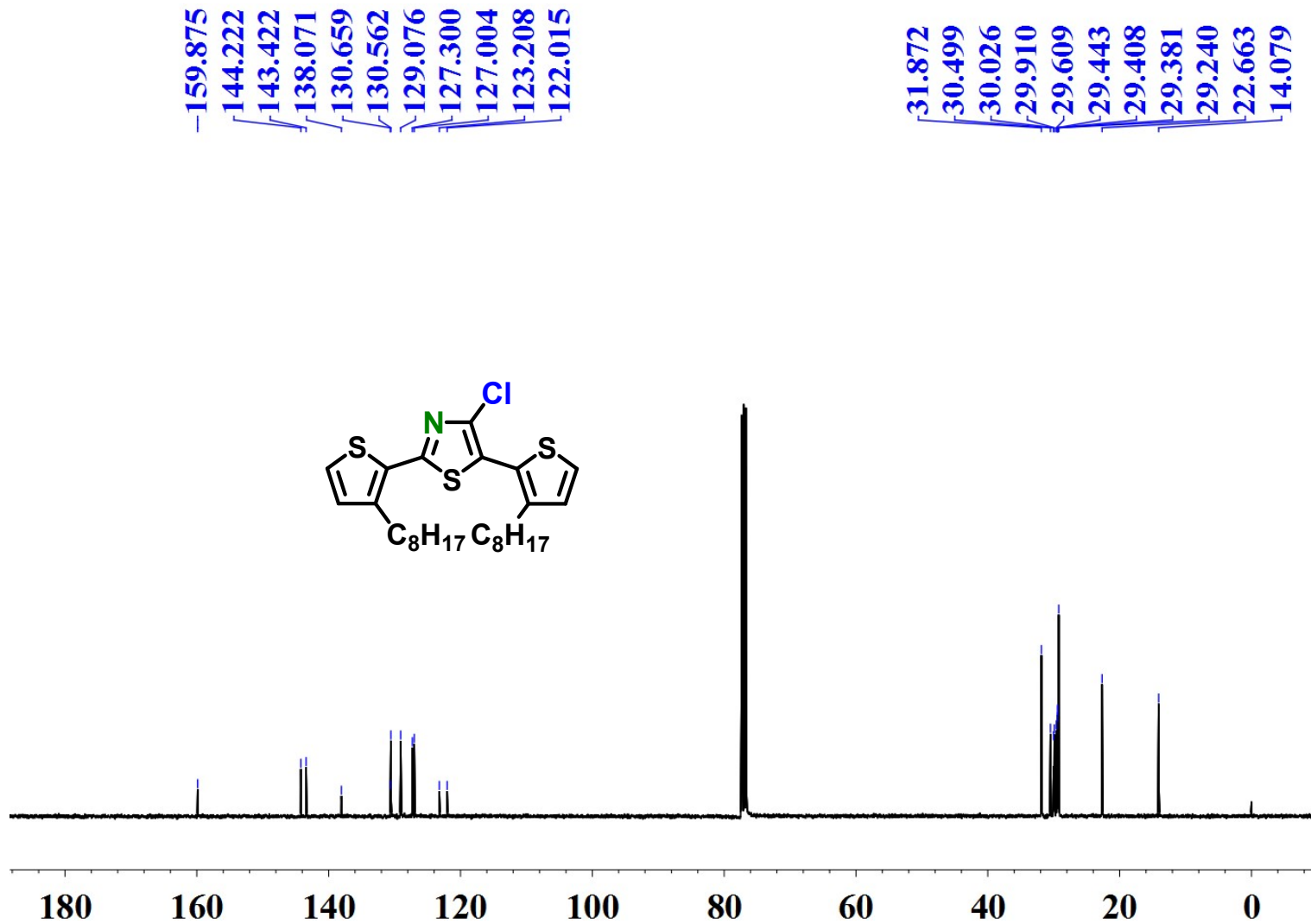


Figure S11. <sup>13</sup>C NMR spectrum of compound 3 in CDCl<sub>3</sub>.

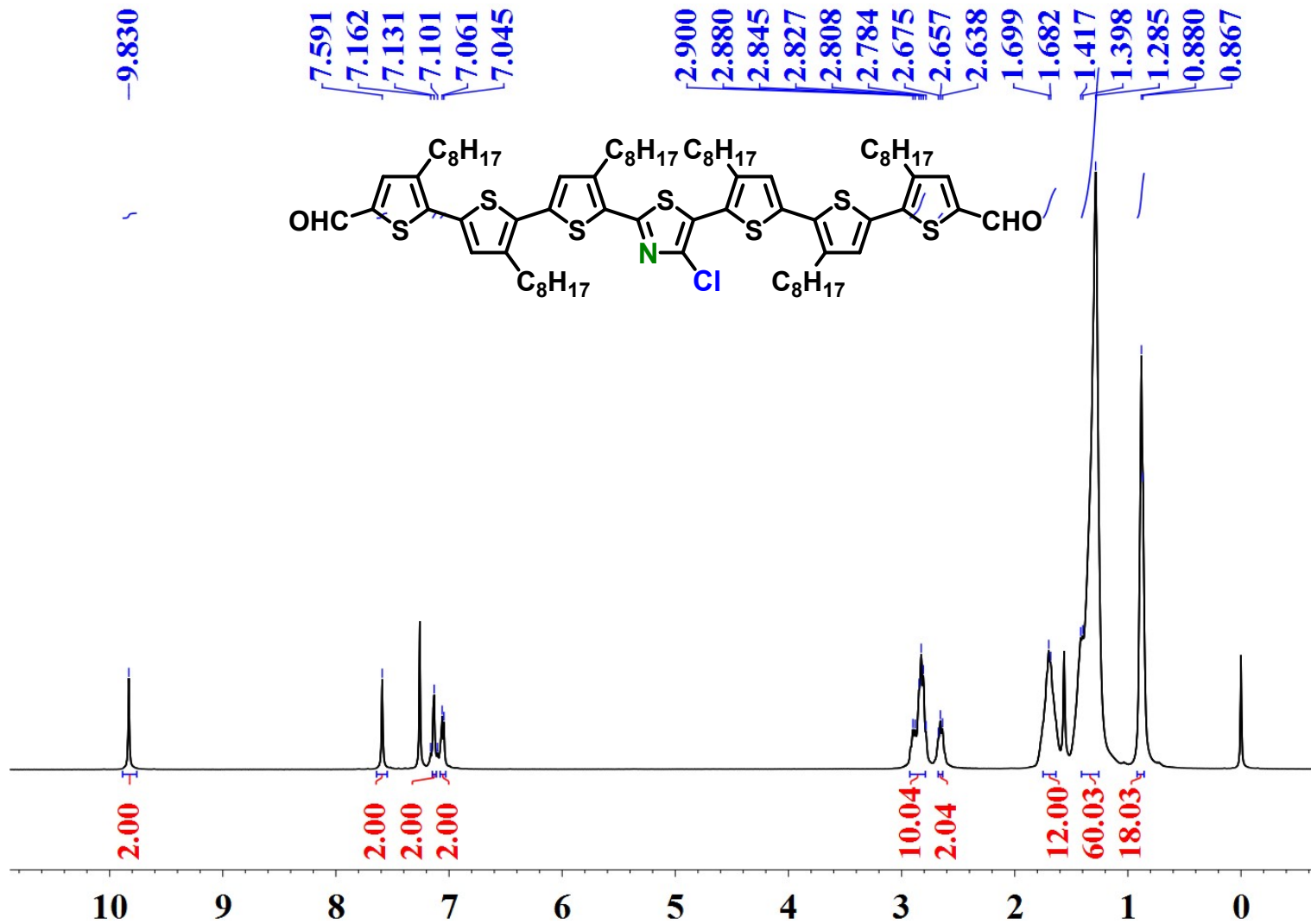


Figure S12. <sup>1</sup>H NMR spectrum of compound 6 in CDCl<sub>3</sub>.

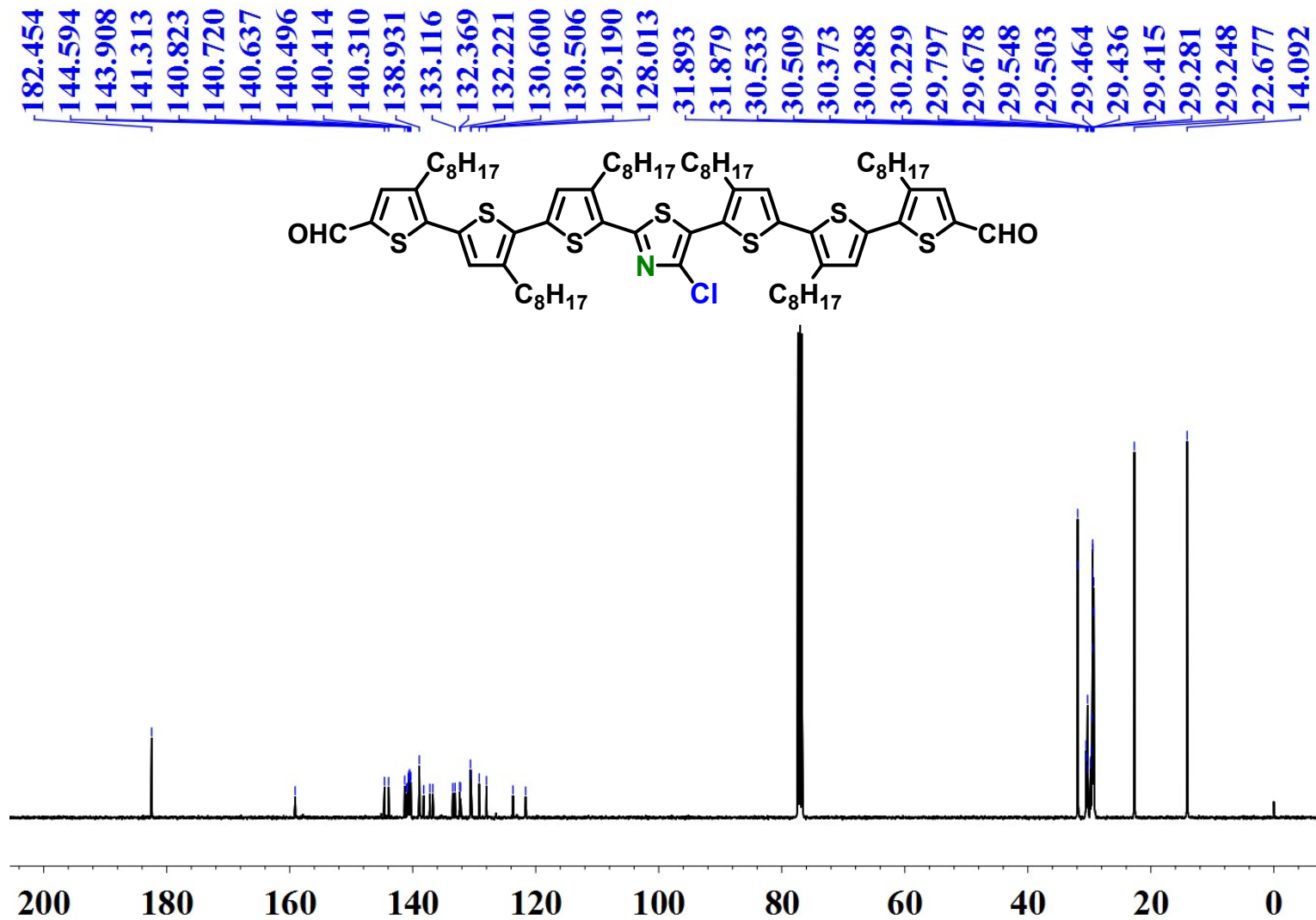


Figure S13.  $^{13}C$  NMR spectrum of compound 6 in  $CDCl_3$

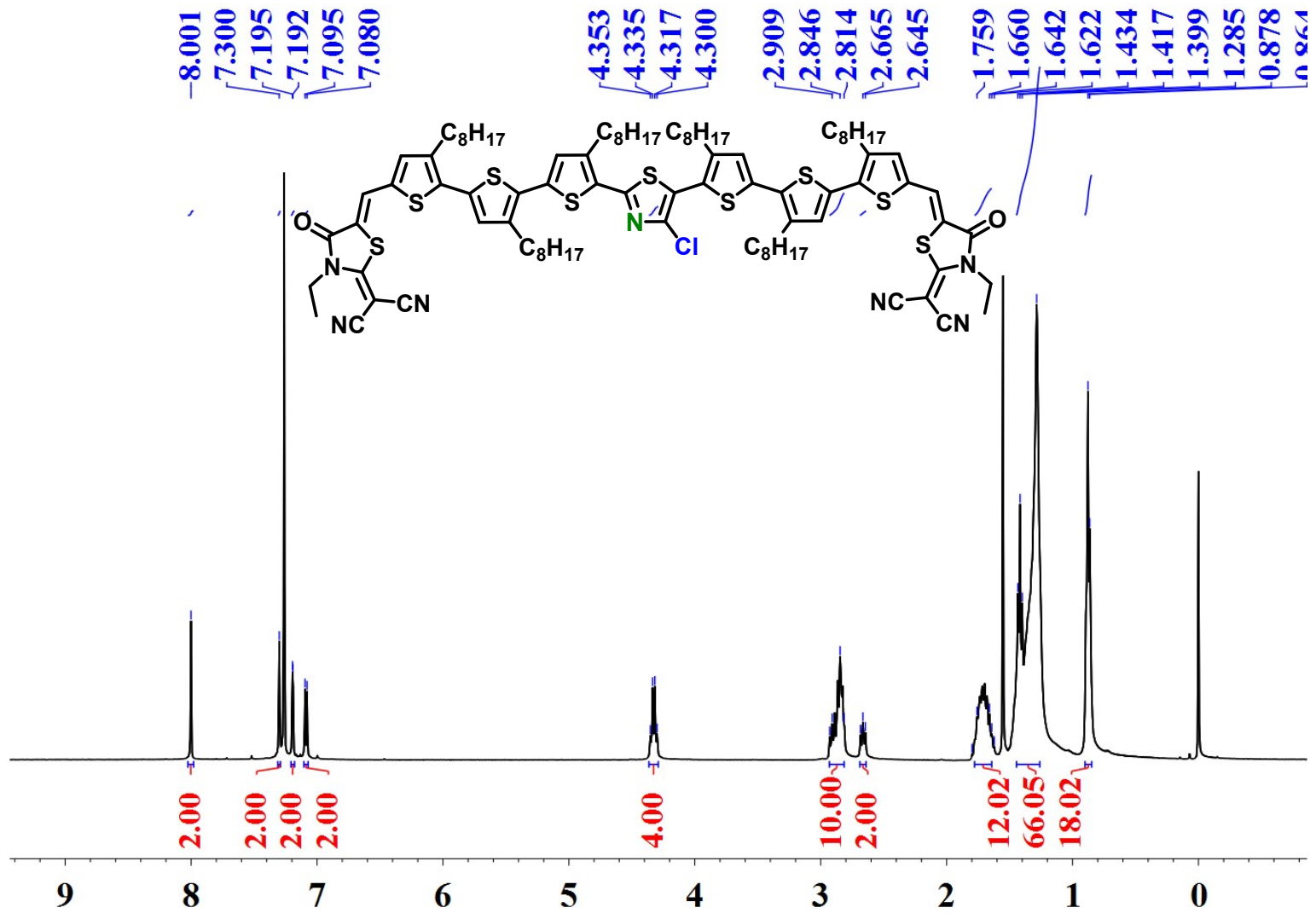


Figure S14. <sup>1</sup>H NMR spectrum of Tz6T in CDCl<sub>3</sub>.

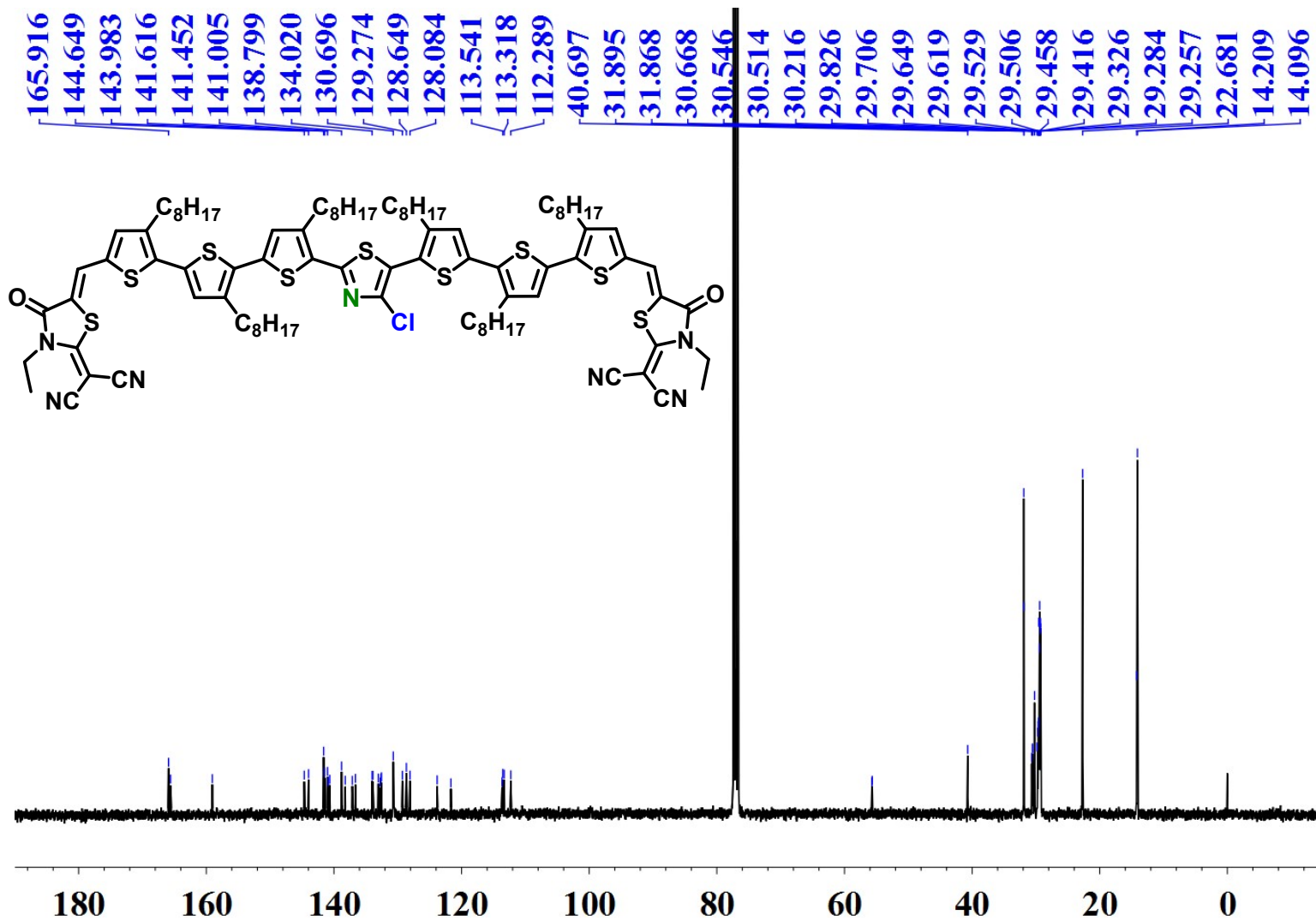
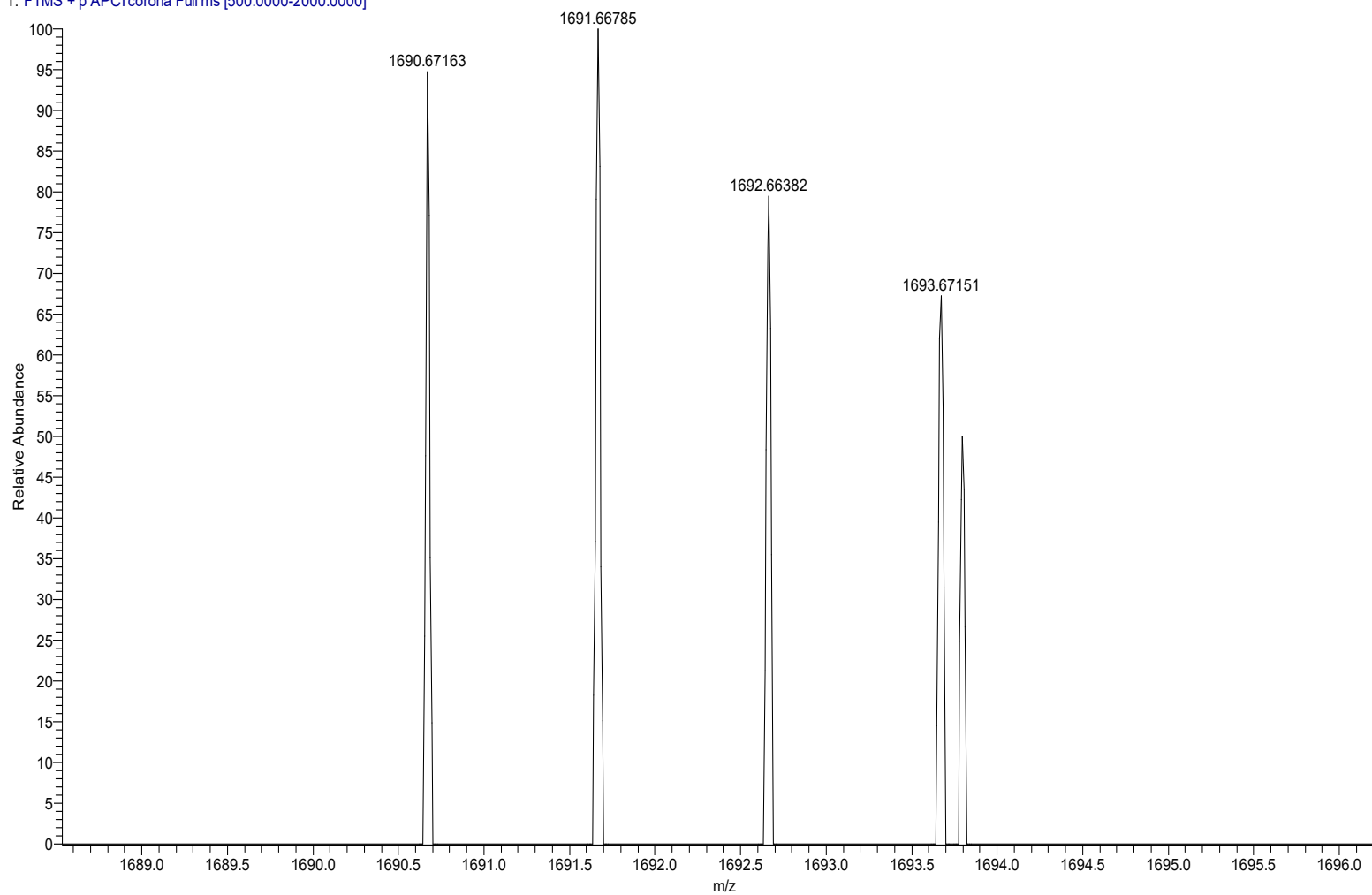


Figure S15. <sup>13</sup>C NMR spectrum of Tz6T in CDCl<sub>3</sub>.

TZ#237 RT: 2.99 AV: 1 NL: 3.64E2  
T: FTMS + p APCI corona Full ms [500.0000-2000.0000]



**Figure S16.** HR-MS spectrum of Tz6T.

**Table S1.** Contact angle of neat films and miscibility parameters of blend films.

Films	Contact Angle (deg)		surface free energy $\gamma$ (mN m <sup>-1</sup> )	absolute difference of $\delta$ ( $\Delta\delta$ , $\times K$ )
	H <sub>2</sub> O	formamide		
2CI7T <sup>a</sup>	100.50 ( $\pm 0.58$ )	78.70 ( $\pm 0.34$ )	24.53	\
eC9-4F <sup>a</sup>	101.09 ( $\pm 0.53$ )	78.85 ( $\pm 0.23$ )	24.80	\
Tz6T <sup>b</sup>	100.85 ( $\pm 0.60$ )	77.16 ( $\pm 0.21$ )	26.77	\
eC9-4F <sup>b</sup>	100.99 ( $\pm 0.43$ )	78.96 ( $\pm 0.30$ )	24.59	\
2CI7T:eC9-4F	\	\	\	0.000738
Tz6T:eC9-4F	\	\	\	0.046

<sup>a</sup> Annealed at 120 °C; <sup>b</sup> Annealed at 150 °C.

**Table S2.** Donor-Acceptor ratio dependence for Tz6T:eC9-4F devices. Performance includes standard deviation across at least 20 devices.

D:A ratio (wt/wt)	$V_{oc}$ (mV)	$FF$ (%)	$J_{sc}$ (mA/cm <sup>2</sup> )	$PCE_{max}$ (%)
1.5:1	868.2	63.16	25.46	13.96
1.8:1	863.4	69.64	25.04	15.05
2.1:1	867.9	70.81	24.03	14.77

**Table S3.** Blend film thickness dependence for Tz6T:eC9-4F devices. Performance includes standard deviation across at least 20 devices.

Thickness (nm)	$V_{oc}$ (mV)	$FF$ (%)	$J_{sc}$ (mA/cm <sup>2</sup> )	$PCE_{max}$ (%)
100	864.9	71.85	23.69	14.72
120	866.0	70.80	24.85	15.12
150	866.6	67.11	24.48	14.23

**Table S4.** Diverse post-condition dependence for Tz6T:eC9-4F devices. Performance includes standard deviation across at least 20 devices..

Temperature	$V_{oc}$ (mV)	$FF$ (%)	$J_{sc}$ (mA/cm <sup>2</sup> )	$PCE_{max}$ (%)
140 °C/5min	871.7	68.18	24.89	14.79
150 °C/5min	863.3	70.86	25.14	15.38
160 °C/5min	859.5	71.32	24.15	14.80

**Table S5.** Packing parameters of neat films, as derived from GIWAXS measurements.

Pure film	Lattice plane	Peak location ( $\text{\AA}^{-1}$ )	d-spacing ( $\text{\AA}$ )	Coherence length ( $\text{\AA}$ )
		$q_{xy}$	$q_{xy}$	$q_{xy}$
<b>2CI7T</b>	010	1.315	4.78	31.46
<b>Tz6T</b>	010	1.333	4.71	17.86
Pure film	Lattice plane	Peak location ( $\text{\AA}^{-1}$ )	d-spacing ( $\text{\AA}$ )	Coherence length ( $\text{\AA}$ )
		$q_z$	$q_z$	$q_z$
<b>2CI7T</b>	010	1.346	4.67	31.24
<b>Tz6T</b>	200	0.485	12.95	71.18
	300	0.734	8.56	24.12

**Table S6.** Packing parameters of blend films, as derived from GIWAXS measurements.

Blend film	Lattice plane	Peak location ( $\text{\AA}^{-1}$ )	d-spacing ( $\text{\AA}$ )	Coherence length ( $\text{\AA}$ )
		$q_z$	$q_z$	$q_z$
<b>2CI7T:eC9-4F</b>	010	1.359	4.62	24.67
<b>Tz6T:eC9-4F</b>	010	1.350	4.65	30.21

**Table S7.** Mobility values of devices of **2CI7T:eC9-4F** and **Tz6T:eC9-4F**.

Blends	$\mu_h (\times 10^{-3} \text{ cm}^2 \text{ V}^{-1} \text{ s}^{-1})$	$\mu_e (\times 10^{-3} \text{ cm}^2 \text{ V}^{-1} \text{ s}^{-1})$	$\mu_h/\mu_e$
<b>2CI7T:eC9-4F</b>	0.74 (0.58±0.15)	1.28 (1.09±0.17)	0.58
<b>Tz6T:eC9-4F</b>	1.30 (1.06±0.22)	1.46 (1.24±0.20)	0.89

**Table S8.** Photovoltaic parameters of optimized ASM-OSCs based on **2CI7T:Y6** and **Tz6T:Y6** blends (Statistical data obtained from at least 20 devices.).

Blends	$V_{oc}$ (mV)	$J_{sc}$ (mA/cm <sup>2</sup> )	FF (%)	PCE (%)
<b>2CI7T:Y6</b>	853.8	19.72	69.24	11.66 (11.45±0.22)
<b>Tz6T:Y6</b>	857.1	23.24	68.06	13.55 (13.39±0.17)

**Table S9.** Properties of 2C17T and Tz6T calculated at relaxed S1 state.  $E_{S1}$ : the transition energy from S0 in eV; **Osc. Str.:** the oscillator strength of S1 state; **D\_idx:** the centroid distance between hole and electron. **Sr:** the overlap integral of hole and electron. **Orb. Comp.:** the orbital composition of the S1 state. **HOMO** and **LUMO:** frontier orbital levels in eV at relaxed S1 geometry.  $E_b$ : the exciton binding energy in eV.  $\mu_{S1}$  and  $\mu_{S0}$ : the dipole moments in Debye.

Mol	$E_{S1}$ (eV)	Osc. Str.	D_idx	Sr	Orb. Comp.
2C17T	1.498	3.958	0.362	0.682	H-L:0.945
Tz6T	1.495	3.816	3.289	0.676	H-L:0.923
Mol	HOMO (eV)	LUMO (eV)	$E_b$ (eV)	$\mu_{S1}$ (Debye)	$\mu_{S0}$ (Debye)
2C17T	-5.153	-3.218	0.438	12.751	10.582
Tz6T	-5.191	-3.259	0.437	15.779	11.133

**Table S10.** Properties of 2C17T/eC9-4F and Tz6T/eC9-4F calculated at relaxed S1 state. Two conformers were calculated for each D/A pair, where D(A)/A(A) indicates the acceptor moiety of the donor molecule stacks with the acceptor moiety of the acceptor molecule stacks and D(A)/A(D) indicates the acceptor moiety of the donor molecule stacks with the donor moiety of the acceptor molecule.  $E_{CT}$ : the transition energy from S0 to S1 in eV. **Orb. Comp.:** the orbital composition of the S1 state. **HOMO** and **LUMO:** frontier orbital levels in eV at relaxed S1 geometry.  $E_b$ : the exciton binding energy.

	$E_{CT}$ (eV)	Orb. Comp.	HOMO (eV)	LUMO (eV)	$E_b$ (eV)
2C17T(A) / eC9-4F(A)	1.099	H-L:0.906	-5.163	-3.729	0.335
2C17T(A) / eC9-4F(D)	1.267	H-L:0.977	-5.176	-3.677	0.232
Tz6T(A) / eC9-4F(A)	1.162	H-L:0.895	-5.209	-3.740	0.306
Tz6T(A) / eC9-4F(D)	1.296	H-L:0.977	-5.190	-3.682	0.213

**Table S11.** Relaxed torsion angle scan data of 2Cl7T and Tz6T.

<b>Angle (°)</b>	<b>Tz6T S0 (kcal/mol)</b>	<b>2Cl7T S0 (kcal/mol)</b>	<b>Tz6T probability</b>	<b>2Cl7T probability</b>	<b>Tz6T S1 (eV)</b>	<b>2Cl7T S1 (eV)</b>
<b>0</b>	0.000	0.387	1.000	1.000	1.990	2.004
<b>10</b>	0.323	0.407	0.000	0.582	1.987	1.998
<b>20</b>	1.023	0.407	0.000	0.180	1.992	2.029
<b>30</b>	1.995	0.425	0.000	0.035	2.005	2.056
<b>40</b>	3.126	0.475	0.000	0.005	2.048	2.090
<b>50</b>	4.418	0.984	0.000	0.001	2.097	2.126
<b>60</b>	4.201	0.054	0.000	0.001	2.178	2.166
<b>70</b>	4.962	0.302	0.000	0.000	2.226	2.214
<b>80</b>	7.003	0.340	0.000	0.000	2.265	2.243
<b>90</b>	7.013	1.809	0.000	0.000	2.257	2.258
<b>100</b>	6.381	1.391	0.000	0.000	2.203	2.253
<b>110</b>	5.338	0.000	0.000	0.000	2.139	2.243
<b>120</b>	4.142	0.265	0.000	0.001	2.083	2.213
<b>130</b>	2.990	0.272	0.000	0.007	2.031	2.178
<b>140</b>	2.093	0.821	0.000	0.030	2.012	2.160
<b>150</b>	1.410	1.915	0.000	0.094	1.982	2.120
<b>160</b>	0.693	3.458	0.000	0.313	1.997	2.090
<b>170</b>	0.519	5.413	0.000	0.419	1.983	2.041
<b>180</b>	0.478	7.274	0.000	0.449	1.971	1.984

**Table S12.** The photovoltaic parameters of oligothiophene donors based OSCs reported in literature.

<b>Donors</b>	<b>Acceptor</b>	$V_{OC}$ (V)	$J_{SC}$ (mA cm <sup>-2</sup> )	<b>FF (%)</b>	<b>PCE (%)</b>	<b>Year</b>
<b>DCN7T</b>	PC <sub>61</sub> BM	0.82	10.23	29.2	2.45 <sup>4</sup>	2010
<b>Compound 2</b>	C <sub>60</sub>	0.51	2.16	28.0	0.36 <sup>5</sup>	2011
<b>Compound 3</b>	C <sub>60</sub>	0.81	3.70	36.0	1.21 <sup>5</sup>	2011
<b>DCAEH7T</b>	PC <sub>61</sub> BM	0.93	9.91	49.1	4.52 <sup>6</sup>	2011
<b>DCAO7T</b>	PC <sub>61</sub> BM	0.86	10.74	55.0	5.08 <sup>6</sup>	2011
<b>DERHD7T</b>	PC <sub>61</sub> BM	0.92	13.98	47.4	6.10 <sup>7</sup>	2012
<b>T3</b>	PC <sub>71</sub> BM	0.85	10.79	67.1	6.15 <sup>8</sup>	2013
<b>DRCN7T</b>	PC <sub>71</sub> BM	0.91	14.87	68.7	9.30 <sup>9</sup>	2015
<b>DRCN5T</b>	PC <sub>71</sub> BM	0.92	15.88	69.0	10.08 <sup>10</sup>	2016
<b>DRCN5T</b>	TPH	1.04	11.59	51.0	6.16 <sup>11</sup>	2016
<b>DRCN5T</b>	IDIC8-F	0.864	15.21	64.1	8.42 <sup>12</sup>	2018
<b>DRCN5T</b>	F-2Cl	0.906	15.97	68.4	9.89 <sup>13</sup>	2018
<b>D5T2F-P</b>	IDIC-4F	0.86	16.85	63.0	9.36 <sup>14</sup>	2020
<b>2F7T</b>	Y6	0.79	20.72	54.1	9.41 <sup>15</sup>	2020
<b>2Cl7T</b>	Y6	0.83	19.69	68.1	11.45 <sup>15</sup>	2020
<b>Tz6T</b>	<b>eC9-4F</b>	<b>0.863</b>	<b>25.14</b>	<b>70.86</b>	<b>15.38</b>	<b>This work</b>

## References

- 1 F. E. Herkes, T. A. Bazer, *J. Heterocyclic Chem.* **1976**, *13*, 1297–1304.
- 2 Y. S. Liu, X. J. Wan, F. Wang, J. Y. Zhou, G. K. Long, J. G. Tian, Y. S. Chen, *Adv. Mater.* **2011**, *23*, 5387–5391.
- 3 J. Pommerehne, H. Vestweber, W. Guss, R. F. Mahrt, H. Bassler, M. Porsch, J. Daub, *Adv. Mater.* **1995**, *7*, 551–554.
- 4 Y. S. Liu, X. J. Wan, B. Yin, J. Y. Zhou, G. K. Long, S. G. Yin, Y. S. Chen, *J. Mater. Chem.* **2010**, *20*, 2464–2468
- 5 D. Demeter, T. Rousseau, P. Leriche, T. Cauchy, R. Po, J. Roncali, *Adv. Funct. Mater.* **2011**, *21*, 4379–4387.
- 6 Y. Liu, X. Wan, F. Wang, J. Zhou, G. Long, J. Tian, J. You, Y. Yang, Y. Chen, *Adv. Energy Mater.* **2011**, *1*, 771–775.
- 7 Z. Li, G. He, X. Wan, Y. Liu, J. Zhou, G. Long, Y. Zuo, M. Zhang, Y. Chen, *Adv. Energy Mater.* **2012**, *2*, 74–77.
- 8 Y. Liu, Y. Yang, C.-C. Chen, Q. Chen, L. Dou, Z. Zhong, G. Li, Y. Yang, *Adv. Mater.* **2013**, *25*, 4657–4662.
- 9 Q. Zhang, B. Kan, F. Liu, G. K. Long, X. J. Wan, X. Q. Chen, Y. Zuo, W. Ni, H. J. Zhang, M. M. Li, Z. C. Hu, F. Huang, Y. Cao, Z. Q. Liang, M. T. Zhang, T. P. Russell, Y. S. Chen, *Nat. Photonics* **2015**, *9*, 35–41;
- 10 B. Kan, M. M. Li, Q. Zhang, F. Liu, X. J. Wan, Y. C. Wang, W. Ni, G. K. Long, X. Yang, H. R. Feng, Y. Zuo, M. T. Zhang, F. Huang, Y. Cao, T. P. Russell, Y. S. Cheng, *J. Am. Chem. Soc.* **2015**, *137*, 3886–3893.
- 11 N. Liang, D. Meng, X. Ma, B. Kan, X. Meng, Z. Zheng, W. Jiang, Y. Li, X. Wan, J. Hou, W. Ma, Y. Chen, Z. Wang, *Adv. Energy Mater.* **2017**, *7*, 1601664.
- 12 Y. Wang, M. Chang, B. Kan, X. Wan, C. Li, Y. Chen, *ACS Appl. Energy Mater.* **2018**, *1*, 2150–2156.
- 13 Y. Wang, Y. Wang, B. Kan, X. Ke, X. Wan, C. Li, Y. Chen, *Adv. Energy Mater.* **2018**, *8*, 1802021.

- 14 T. N. Duan, J. Gao, M. Babics, Z. P. Kan, C. Zhong, R. Singh, D. H. Yu, J. W. Lee, Z. Y. Xiao, S. R. Lu, *Solar RRL* **2020**, *4*, 1900472.
- 15 T. N. Duan, J. Gao, T. L. Xu, Z. P. Kan, W. J. Chen, R. Singh, G. P. Kini, C. Zhong, D. H. Yu, Z. G. Xiao, Z. Y. Xiao, S. R. Lu, *J. Mater. Chem. A*, **2020**, *8*, 5843-5847.